



A metabonomic approach to the effect evaluation of treatment in patients infected with influenza A (H1N1)

Chuanjian Lu^{a,*}, Zhiting Jiang^{b,c,1}, Xuemei Fan^b, Guiya Liao^a, Shasha Li^a, Chunxia He^a, Ling Han^a, Shijuan Luo^a, Yixin Liu^a, Huangguo Lin^a, Li Li^a, Xue Li^{a,b}, Qionglin Liang^{a,b}, Yiming Wang^{a,b}, Guoan Luo^{a,b,**}

^a Guangdong Provincial Hospital of Traditional Chinese Medicine, Guangzhou, PR China

^b Key Laboratory of Bioorganic Phosphorus Chemistry & Chemical Biology, Department of Chemistry, Tsinghua University, Beijing, PR China

^c School of Pharmacy, East-China University of Science & Technology, Shanghai, PR China

ARTICLE INFO

Article history:

Received 24 April 2012

Received in revised form

26 July 2012

Accepted 30 July 2012

Available online 21 August 2012

Keywords:

H1N1

Metabonomics

UPLC/TOF MS

Potential biomarker

ABSTRACT

The pandemic influenza A virus (H1N1) was transmitted to the human population since 2009, resulting in some consequences of viral pneumonia, respiratory failure, multiple organ failure and, most severely, death. In clinical practice, Chinese medicine possessed extensive experience for prevention and treatment of influenza, but its mechanism still remain unclear. In addition, the efficacy of combination therapy of Chinese and Western medicine was attractive, but not yet clear. In the present study, 131 patients from Guangzhou China referred for H1N1 virus mRNA testing for the evaluation of possible influenza A-infected were eligible for participation. A metabonomics study was carried out to explore the difference between before and after treatment in patients with H1N1 through Chinese and/or Western medicine. Results from metabolic profiling and biochemical detection indicated significant metabolic change in the arachidonic acid metabolic pathway. In the group of combination therapy of Chinese and western medicine, its efficacy was best and the potential biomarkers were significantly changed compared with untreated state. Those results indicated that the potential metabolic biomarker could be supplemented with biochemical detection to obtain more precise diagnosis for H1N1 infection.

Clinical trials registration: Clinical Trials. Gov No. 2008GL-50

© 2012 Elsevier B.V. All rights reserved.

1. Introduction

On June 11, 2009, the World Health Organization (WHO) announced that the rapid global spread of a strain of influenza A (H1N1) virus detected the previous week warranted moving the global pandemic alert level to phase 6, indicating that the episode of influenza had entered a pandemic stage [1,2]. As of December 7, 2009, 4328 severe cases of pandemic influenza H1N1 were reported in Mainland China, including at least 326 deaths [3]. Initial cases of pandemic influenza H1N1 were characterized by fever, cough and throat congestion, with elevated C-reaction protein (CRP) and neutrophils as the most significant lab findings. The pandemic influenza H1N1 strain was able to affect multiple organs, and thus interfere with several biological processes [4]. Although several

biomarkers accurately can diagnose patients with pandemic influenza, there is no report showing the change in metabolism of patients infected by H1N1 virus after the treatment.

Recently, there have been technical advances that have allowed extremely high-density data sets to be constructed from individuals. There are three methods most promising of wide application in diagnostic biochemical profiling, namely Nuclear Magnetic Resonance (NMR) spectroscopy [5,6], Liquid Chromatography [7], and Mass Spectrometry [8,9].

Liquid Chromatography coupled with electrospray mass spectrometry has been used in the research of a variety of diseases in our previous work, such as diabetic nephropathy [10] and neural tube defects [11]. In this study, we have applied recently developed pattern recognition techniques to MS spectra of serum taken from individuals who have been extensively characterized for the presence of H1N1 virus infection by detecting influenza A virus mRNA. This protocol is performed in patients both before and after a reversible virus injury, and thus allowing each patient to serve as his own biological control. The purpose of this study is to identify and characterize the changes of specific metabolic pathways and circulating metabolites between the H1N1 virus

* Corresponding author at: Tel./fax: +86 20 8188365.

** Corresponding author at: Department of Chemistry, Tsinghua University, Beijing 100084, PR China. Tel./fax: +86 10 62781688.

E-mail addresses: luchuanjian888@vip.sina.com (C. Lu), luoga@mail.tsinghua.edu.cn (G. Luo).

¹ These two authors contributed equally to the paper.

infection and its reversible recover. Such metabolites might ultimately serve as targets for therapeutic intervention, and also be used as substrates for molecular imaging. Furthermore metabolic profiling could be a useful method applied to diagnose adjunctively patients with H1N1 virus.

2. Experimental

2.1. Patients and methods

All 131 patients who were referred for H1N1 virus mRNA testing for the evaluation of possible influenza A-infected were eligible for participation, and they were diagnosed by influenza A (H1N1) virus mRNA detection at their first visit to the Guangdong Provincial Hospital of Traditional Chinese Medicine. Patients with positive viral nucleic acid were recognized as patients with H1N1 virus infection, and when their viral nucleic acid turning negative after treatment were classed in the group of patients after treatment. The Institutional Ethics Committee of Guangdong Provincial Hospital of Traditional Chinese Medicine approved the study protocol (No. 2008GL-50), and all patients provided written informed consent. Patients who underwent pharmacological testing were excluded.

Data obtained include each patient's age, sex, height, weight, blood routine and biochemical indicator reflected hepatic, kidney and heart functions were also collected to check the tissue condition.

2.2. UPLC and MS analysis

Thawed serum samples (100 μ L) were mixed with methanol (400 μ L) by vortexing for 2 min, and then centrifuged at 4 $^{\circ}$ C for 15 min at 13,000 rpm. The supernatant was transferred to a 1.5 mL polypropylene tube, diluted with 500 μ L of ultrapure water, and then filtered through a syringe filter (0.22 μ m) for UPLC-TOF MS analysis.

Serum metabolite profiling was performed with UPLC-MS. Chromatography was carried out with an ACQUITY BEH C₁₈ chromatography column (2.1 \times 100 mm, 1.7 μ m). The column temperature was maintained at 50 $^{\circ}$ C, and then binary mobile phase was composed of phase A (water with 0.1% formic acid) and phase B (acetonitrile).

The gradient for the serum sample was: 0–3 min, 5–50% B; 3–7 min, 50–70% B; 7–12 min, 70–95% B; 12–14 min, following by washing with 95% B. The proportion of phase B returned to 5% in 1 min, and the column was allowed to re-equilibrate for 5 min before the next injection. The flow rate was 0.4 mL/min, and 6 μ L was injected into the column.

For MS we used the W mode of operation and negative ion electrospray mode. The capillary voltage was set at 2300 V, and cone voltage at 35 V. Nitrogen was used as the dry gas, the desolvation gas flow rate was set at 600 L/h, and cone gas flow was maintained at 40 L/h. The desolvation temperature was set at 350 $^{\circ}$ C, and source temperature at 120 $^{\circ}$ C. The scan time and inter-scan delay were set to 0.1 s and 0.02 s, respectively. The TOF data were collected from m/z 50 to 1500. All the data were acquired using an independent reference lock mass via the LockSprayTM interface to ensure accuracy and reproducibility. Leucine enkephalin was used as the reference compound ([M–H][–] = 554.2615) at a concentration of 50 μ g/ μ L under a flow rate of 10 μ L/min. The data were collected in the centroid mode, and the LockSpray frequency set at 10 s and averaged over 10 scans for correction.

2.3. Statistical analysis

Continuous variables were compared with Student's *t* test, and categorical variables were compared with Fisher's exact test. Metabolites for which the distribution of the logarithmically transformed levels in the study population had absolute values of skewness and kurtosis < 1 and a no significant Wilkes–Shapiro test were deemed to have a normal distribution and analyzed with parametric tests; metabolites for which the distribution failed to meet these criteria were analyzed with nonparametric tests. The significance of the change in logarithmically transformed metabolite levels from pretest to posttest values was assessed by paired Student's *t* tests or Wilcoxon signed-rank tests, as appropriate. Data were expressed as means \pm standard deviation (SD).

Software SIMCA (version P12, Umetrics, Umea, Sweden) was used throughout by multivariate data analysis. A 7-fold cross-validation was used for the model building and the evaluation of the significant components.

3. Results and discussion

A total of 131 patients undergoing treatment with H1N1 virus infection served as the study population. The characteristics and biochemistry test performance parameters for these patients are listed in Table 1.

The data obtained from UPLC tandem with time of flight mass spectrometer of human serum from patients with H1N1 virus infection ($n=131$) and their serum after treatment ($n=131$) were compared (Fig. 1). To determine whether it was possible to distinguish patients with H1N1 virus infection and patients after treatment, we carried out principal component analysis (PCA) and partial least squares-discriminant analysis (PLS-DA). PCA is a bilinear decomposition method used for over viewing 'clusters' within multivariate data. PLS-DA is a multivariate classification method based on PLS, the regression extension of PCA [12].

Table 1
Patients characteristics.

Index	Male ($n=66$)	Female ($n=65$)
Characteristics		
Age (year)	23.26 (6.34)	26.17 (9.62)
Height (cm)	170.29 (7.26)	159.09 (4.37)
Weight	60.41 (10.29)	49.97 (6.00)
Routine blood testing		
Leukocyte ($\times 10^9/L$)	7.33 (1.87)	6.31 (1.61)
Neutrophil ($\times 10^9/L$)	5.48 (1.72)	4.64 (1.48)
Lymphocyte ($\times 10^9/L$)	1.10 (0.46)	1.03 (0.44)
Hemoglobin (g/L)	157.44 (47.89)	131.35 (12.65)
Erythrocyte ($\times 10^9/L$)	5.22 (0.72)	4.47 (0.42)
Thrombocyte ($\times 10^{12}/L$)	194.30 (42.09)	198.69 (47.08)
Hepatic functions		
ALT (IU/L)	23.97 (13.13)	17.38 (15.15)
AST (IU/L)	24.71 (8.62)	22.34 (14.88)
Kidney functions		
Urea nitrogen (mmol/L)	4.20 (1.14)	3.38 (0.67)
Creatinine (mmol/L)	95.03 (16.30)	68.94 (10.96)
Heart functions		
Creatine kinase (IU/L)	148.06 (83.56)	81.47 (30.64)
CKMB (IU/L)	17.32 (12.69)	14.86 (6.27)
Immunizing antigen testing		
CD3	55.62 (9.91)	58.12 (9.10)
CD4	27.80 (6.73)	30.64 (7.64)
CD8	21.54 (6.62)	20.99 (6.26)
C reactive protein (mg/L)	15.28 (9.85)	13.05 (11.37)

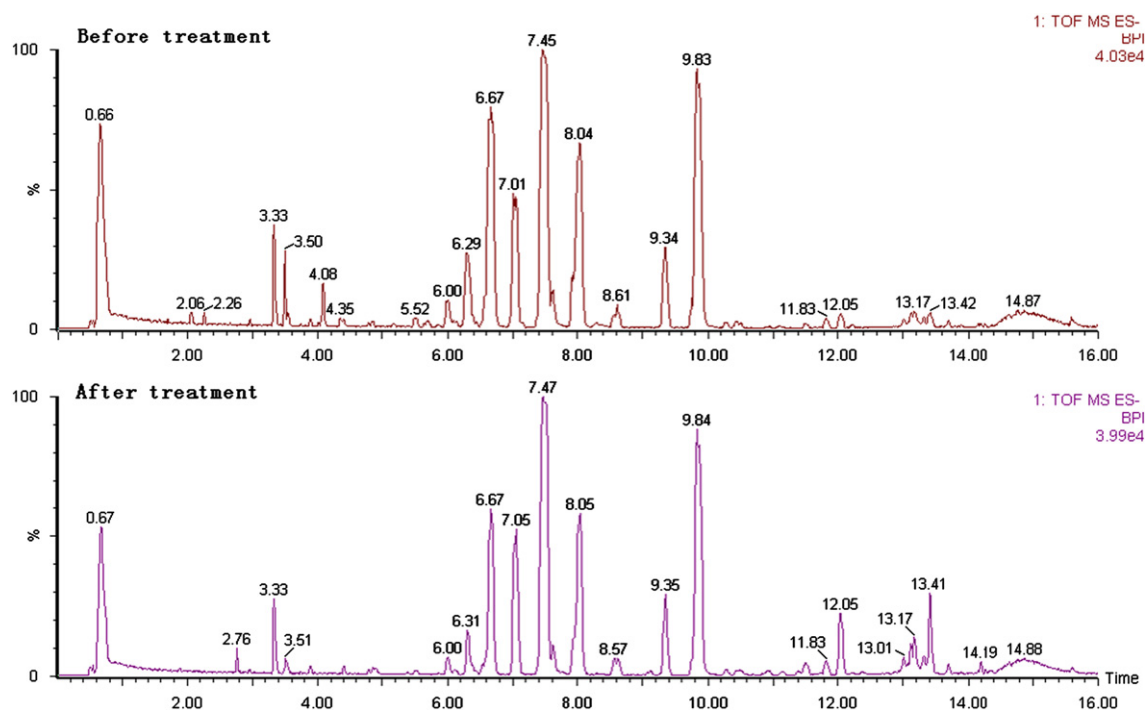


Fig. 1. Serum metabolic profiling of H1N1 patients before and after treatment.

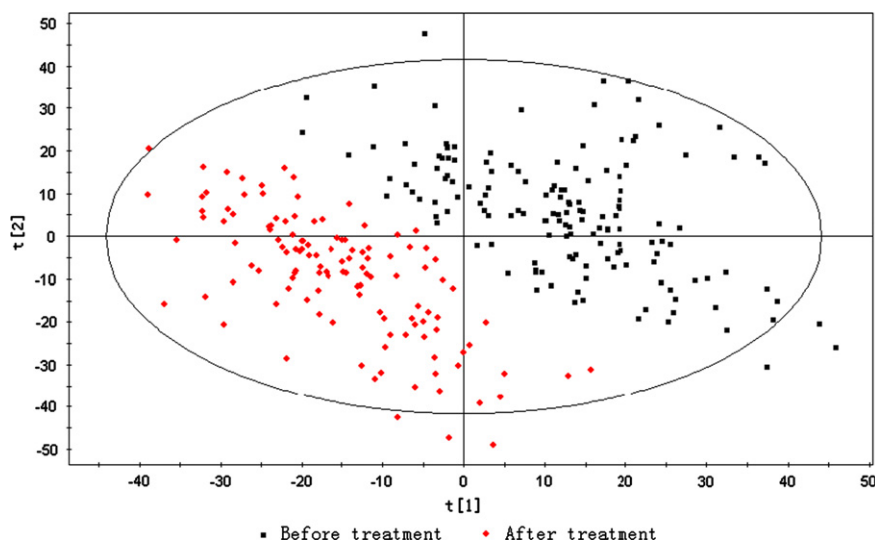


Fig. 2. PLS-DA score plot of patients before and after treatment.

There is no significant difference in PCA plot between two groups (before and after treatment), therefore PLS-DA was used for the analysis of the metabolomics data.

The PLS-DA score plot of the first and second principal components (PC1 and PC2) showed that although there was overlap between the two sample classes, some clustering was evident (Fig. 2). The VIP list of exact mass/retention time pairs obtained from PLS-DA was further confirmed by the software MassLynx (Waters, England). Some parameters, such as deviation from calculated mass (mDa or ppm), double bond equivalent (DBE), and *i*-fit value (the isotopic pattern of the selected ion) were used to evaluate the accuracy of possible formulas. Taking these parameters into account, the confidence of the tentative marker assignment to the candidate was enhanced by the high mass accuracy and low *i*-fit value.

Sequentially, the candidate compound was input in the KEGG ligand (<http://www.genome.jp/kegg/ligand.html>), and the candidate compounds were further confirmed by its authentic standards. Here, we take the ion of *m/z* 135.0354 as an example to illustrate the biomarker identification process. After MassLynx and KEGG analysis, the ion of *m/z* 135.0354 obtained from UPLC-MS was preliminarily defined as homocysteine. Furthermore, under the same chromatography condition, its authentic standard (Sigma) was injected to UPLC-MS, at the same retention time and accurate molecular weight was found and consistent with the result of metabolic fingerprint analysis. Finally, the ion of *m/z* 135.0354 was conformed as homocysteine. Using this iterative approach, compounds listed in Table 2, were identified and considered as potential markers related to the H1N1 virus infection recovery.

Table 2
Potential biomarkers identified related with H1N1 virus infection.

No.	m/z	Ion	Formula	Identification	Metabolic pathway
1	455.2342	[M+COOH] ⁻	C ₂₃ H ₃₇ NO ₆ S	20-OH-LTE4	Arachidonic acid metabolism
2	457.1710	[M+COOH] ⁻	C ₂₀ H ₂₃ N ₇ O ₆	5,10-Methylene-THF	One carbon metabolism
3	505.0165	[M+COOH] ⁻	C ₁₁ H ₁₈ N ₅ O ₁₂ P ₃	α,β-Methylene ATP	
4	368.2199	[M+COOH] ⁻	C ₂₀ H ₃₂ O ₆	PGG2	Arachidonic acid metabolism
5	166.0491	[M-H] ⁻	C ₆ H ₆ N ₄ O ₂	Methylxanthine	
6	370.2355	[M-H] ⁻	C ₂₀ H ₃₄ O ₆	PGF1α	Arachidonic acid metabolism
7	310.2872	[M+COOH] ⁻	C ₂₀ H ₃₈ O ₂	Prostanoic acid	
8	191.0616	[M-H] ⁻	C ₇ H ₁₃ NO ₃ S	N-Acetylmethionine	
9	498.1090	[M+COOH] ⁻	C ₁₆ H ₂₆ N ₄ O ₁₀ S ₂	Glutanyl-L-cysteine	Glutathione metabolism
10	496.2607	[M+COOH] ⁻	C ₂₅ H ₄₀ N ₂ O ₆ S	LTD4	Arachidonic acid metabolism
11	278.2246	[M+COOH] ⁻	C ₁₈ H ₃₀ O ₂	Linolenic acid	Linolenic acid metabolism
12	318.2195	[M+COOH] ⁻	C ₂₀ H ₃₀ O ₃	LTA4	
13	159.0532	[M-H] ⁻	C ₆ H ₉ NO ₄	Methylene-l-glutamate	
14	515.2917	[M+COOH] ⁻	C ₂₆ H ₄₅ NO ₇ S	Taurocholate	Taurine and hypotaurine metabolism
15	370.2355	[M+COOH] ⁻	C ₂₀ H ₃₄ O ₆	6-keto-PGF1α	Arachidonic acid metabolism
16	737.32	[M-H] ⁻	C ₂₈ H ₅₁ N ₉ O ₁₀ S ₂	Homotrypanthione	Glutathione metabolism
17	178.0412	[M-H] ⁻	C ₅ H ₁₀ N ₂ O ₃ S	Cys-Gly	Glutathione metabolism
18	181.0739	[M-H] ⁻	C ₉ H ₁₁ NO ₃	Tyrosine	Tyrosine metabolism
19	135.0354	[M+COOH] ⁻	C ₄ H ₉ NO ₂ S	Homocysteine	Cysteine and methionine metabolism
20	366.2042	[M+COOH] ⁻	C ₂₀ H ₃₀ O ₆	20-COOH-LTB4	Arachidonic acid metabolism
21	111.0433	[M-H] ⁻	C ₄ H ₅ N ₃ O	Cytosine	Pyrimidine metabolism
22	398.1372	[M-H] ⁻	C ₁₅ H ₂₂ N ₆ O ₅ S	SAM	Cysteine and methionine metabolism
23	305.0413	[M+COOH] ⁻	C ₉ H ₁₂ N ₃ O ₇ P	cyclic CMP	
24	213.0038	[M-H] ⁻	C ₄ H ₈ NO ₇ P	Phospho-L-aspartate	Cysteine and methionine metabolism
25	180.0634	[M-H] ⁻	C ₆ H ₁₂ O ₆	Glucose	Pentose phosphate metabolism
26	347.0631	[M-H] ⁻	C ₁₀ H ₁₄ N ₅ O ₇ P	AMP	Purine metabolism
27	467.9736	[M-H] ⁻	C ₉ H ₁₅ N ₂ O ₁₄ P ₃	dUTP	Pyrimidine metabolism
28	381.2644	[M-H] ⁻	C ₁₈ H ₄₀ NO ₅ P	Sphinganine 1-phosphate	
29	177.0640	[M-H] ⁻	C ₆ H ₁₁ NO ₃ S	N-formyl-L-methionine	Cysteine and methionine metabolism
30	301.2981	[M+COOH] ⁻	C ₁₈ H ₃₉ NO ₂	Sphinganine	Sphingolipid metabolism

3.1. Functional pathway analysis

A number of metabolic databases are available electronically, some with features for querying and visualizing metabolic pathways and regulatory networks. We present a unifying, systematic approach based on the KEGG database for storing, displaying, comparing, searching and simulating such nets from a number of different sources. Information of each potential biomarker is extracted and compiled into a KEGG databases, which then be allowed to investigate the (differential) content in metabolic databases, to map and integrate metabonomic information and functional annotations, to compare sequence and metabolic databases with respect to their functional annotations, and to define, generate and search paths and pathways in nets. Finally, arachidonic acid metabolism was significantly overrepresented in the list of potential biomarkers. The relationship of them shown in Fig. 3.

The role of arachidonic acid metabolism in the specific effects of interleukin 1 (IL 1), induction of interleukin 2 (IL 2), and also IL 2 stimulation of proliferation and interferon-gamma (IFN-gamma) production were reported [13]. Utilizing cell lines that are specifically responsive to IL 1 or IL 2, it was found that both interleukins stimulate lipoxygenation of arachidonic acid in their respective target cell. The ability of each interleukin to induce monohydroxyeicosatetraenoic acid (HETE) correlated with the induction of secondary lymphokine secretion [14]. Utilizing selective and partially selective pharmacologic inhibitors of arachidonic acid metabolism, the data suggest that the participation of lipoxygenase activity is required for both IL 1, induction of IL 2 production and IL 2 regulation of proliferation and IFN-gamma secretion. Studies performed with an endogenous inhibitor of 5-lipoxygenase demonstrated the requirement of this enzyme system for IL 2-dependent proliferation and IFN-gamma production. Although leukotrienes could replace IL 2 for IFN-gamma secretion, they had no effect on IL 2 growth promotion. Both IL 1 and IL 2 may share the

lipoxygenase pathway of arachidonic acid metabolism which is a component of the intracellular signal transduction process that regulates secretory activity and cellular proliferation [15].

3.2. Potential biomarkers and the relationship with H1N1 virus

Methylxanthine has been shown to have a variety of effects on hematopoietic cell activation and function. After treatment, methylxanthine was significantly increased in the patients with H1N1 virus infection. These compounds can inhibit cAMP-specific phosphodiesterase activity, resulting in increased levels of intracellular cAMP. AMP was detected increased in our experiment, which well agree with the hypothesis. The effect of methylxanthine was also found on the responses of both mouse and human lymphocytes to stimulation with polyclonal T- and B-cell mitogens, antigens, and the microbial superantigen, staphylococcal enterotoxin B (SEB) [16]. These compounds also inhibited the proliferative responses of human lymphocytes to phytohemagglutinin, SEB, and tetanus toxoid. Efforts to determine whether these methylxanthine compounds mediated their inhibitory effects through a specific protein kinase pathway revealed a role for cAMP-dependent protein kinase A in methylxanthine-induced immunomodulation [17].

Cysteinyl leukotrienes (CysLT) are potent lipid mediators, synthesized from nuclear membrane arachidonic acid in numerous cell types via the 5-lipoxygenase pathway and have principal pathophysiological roles in asthma and allergic rhinitis [18]. Apart from acting as potent bronchoconstrictors and pro-inflammatory mediators, increasing evidence suggests for CysLT a much broader spectrum of pathophysiological functions [19], including CysLT's contribution to airway remodeling also by their direct effects on lung mesenchymal cells [20–23]. CysLT mediate their diverse effects through at least two G-protein coupled receptors (GPCRs), CysLT1 and CysLT2 [23]. LTD4 exert its effect primarily through receptors CysLT1, which is similar to CXCR4 chemokine receptors.

LTA4 hydrolase is a zinc containing enzyme, which stereospecifically catalyzes the hydrolysis of the epoxide LTA4 to the diol LTB4. There is a substantial evidence that LTB4 plays a significant role in the amplification of many inflammatory disease states. Therapeutic agents which selectively inhibit LTA4 hydrolase would block the formation of LTB4 and thus be potentially useful for the treatment of inflammation [24]. Numerous inhibitors of LTA4 hydrolase have

been reported over the past 15–20 years. Several early inhibitors were based on the structure of the natural substrate, LTA4. Later approaches utilized known inhibitors of related zinc containing metalloproteinases and led to the identification of captopril, bestatin and kelatorphan as potent inhibitors of LTA4 hydrolase. The change of these CysLTs and their metabolites in the arachidonic acid pathway was also shown in Fig. 4.

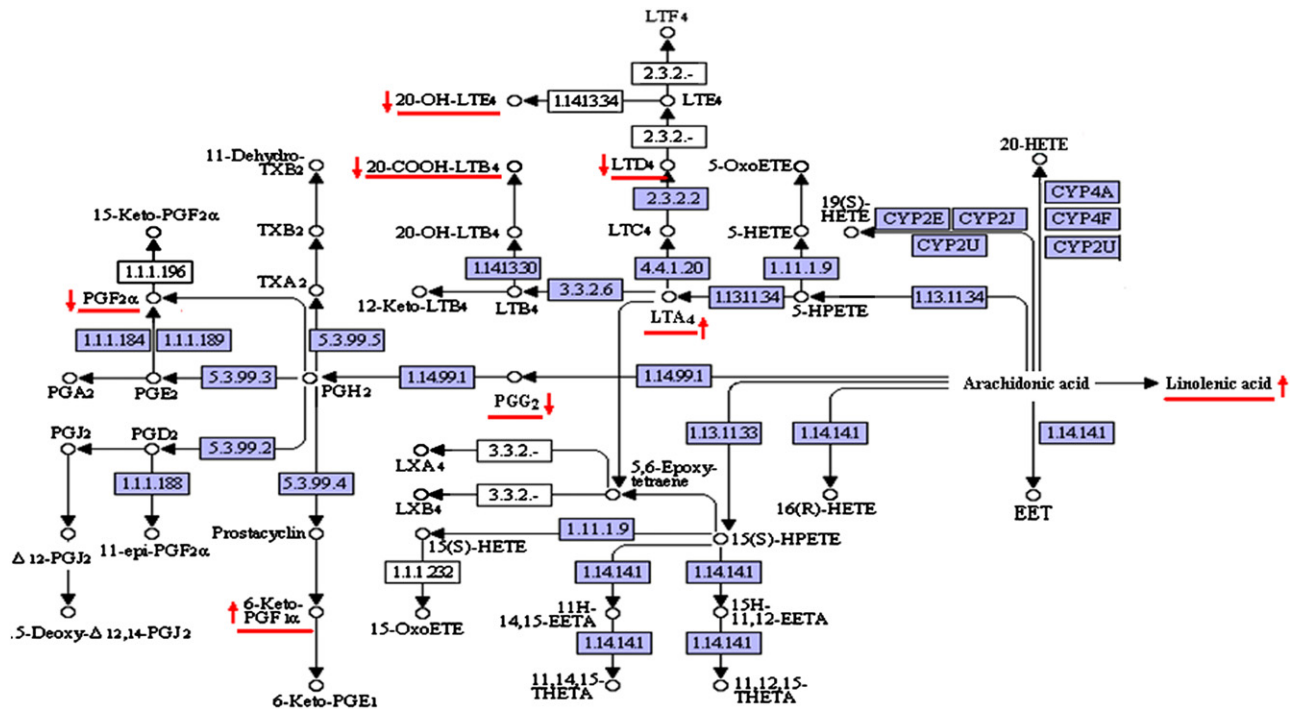


Fig. 3. Arachidonic acid metabolism and some potential biomarkers changed in this pathway.

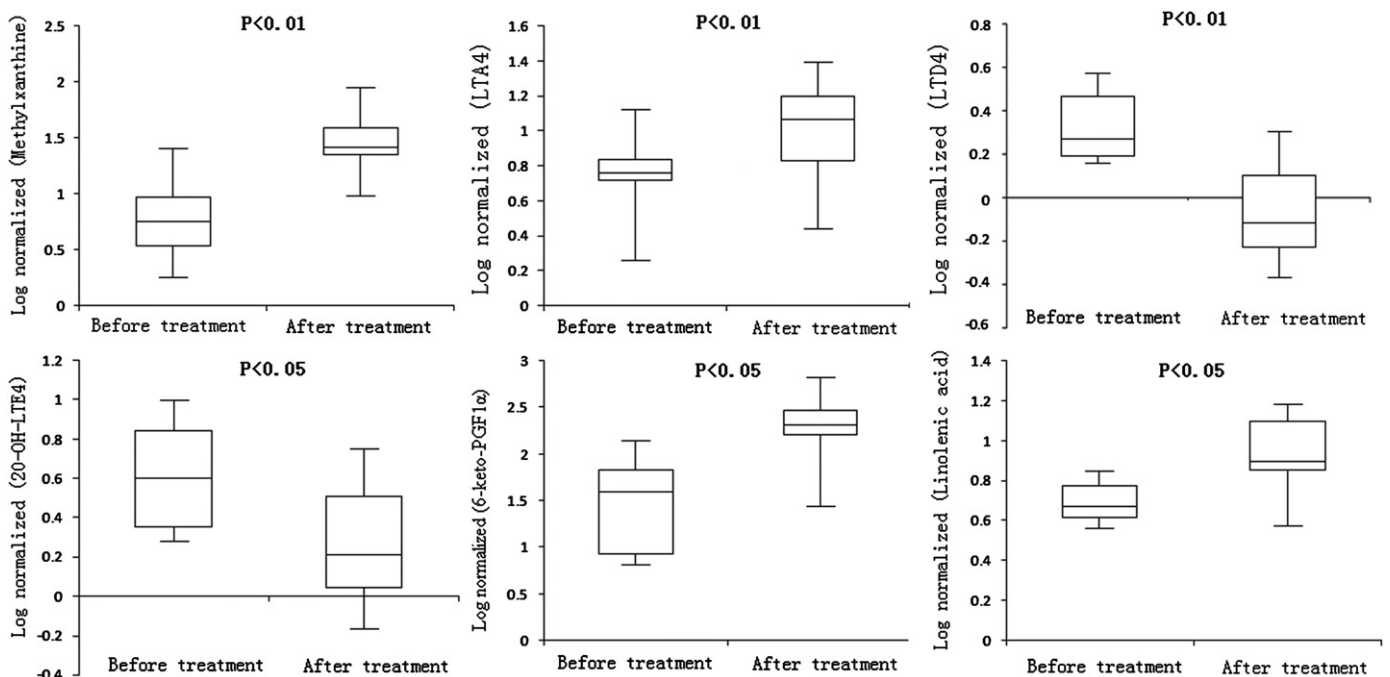


Fig. 4. Box-and-whisker plots of the changes seen after treatment in six metabolites in two groups. The line in the box represents the median change in the normalized logarithm value; the lower and upper boundaries of the box represents the 25th and 75th percentiles, respectively; the lower and upper whiskers represent the 5th and 95th percentiles; *P* values shown at the top measure the significant difference in the change between two groups.

4. Conclusion

In summary, metabolite profiling using UPLC-TOF MS integrated with modern multivariate statistical techniques was successfully applied to simultaneously monitor multi-metabolic pathways affected by H1N1 virus. Biochemical analysis showed that H1N1 virus also affected the immune system, as patients showed elevated CRP and an overall decrease in CD3 and CD4 levels. These findings indicate that the pandemic influenza H1N1 strain can spread to multiple organs. The results from metabolomics study showed methylxanthine and some CysLTs in patients significantly changed after treatment, which induced to immunomodulation in the body. Arachidonic acid metabolism is the key metabolic pathway related with the treatment of H1N1 virus, metabolites of which have modulatory effects on the development of cellular immunity.

Acknowledgments

This study was supported by the National Special Program of TCM of China: Clinical Research on H1N1 Pandemic Influenza Treated with TCM. (No. 200907001-2B).

References

- [1] World Health Organization. Epidemic and Pandemic Alert and Response (EPR). Available at: <<http://www.who.int/csr/disease/swineflu/en/index.html>>, (accessed 24.06.09), 2009.
- [2] V. Trifonov, H. Khiabani, R. Rabadan, N. Engl. J. Med. 361 (2009) 115–119.
- [3] World Health Organization. Pandemic (H1N1) 2009-update 79. Available at: <http://www.who.int/csr/don/2009_12_18a/en/index.html>, (accessed 18.12.12), 2009.
- [4] Y.P. Mu, Z.Y. Zhang, X.R. Chen, X.H. Xi, Y.F. Lu, Y.W. Tang, H.Z. Lu, Q. J. Med. 103 (2010) 311–317.
- [5] L.M. Raamsdonk, B. Teusink, D. Broadhurst, N.S. Zhang, A. Hayes, M.C. Walsh, J.A. Berden, K.M. Brindle, D.B. Kell, J.J. Rowland, H.V. Westerhoff, K. Dam, S.G. Oliver, Nat. Biotechnol. 19 (2001) 45–50.
- [6] J.T. Brindle, H. Antti, E. Holmes, G. Tranter, J.K. Nicholson, H.W.L. Bethell, S. Clarke, P.M. Schofield, E. McKilligin, D.E. Mosedale, D.J. Grainger, Nat. Med. 8 (2002) 1439–1444.
- [7] K.E. Vigneau-Callahan, A.I. Shestopalov, P.E. Milbury, W.R. Matson, B.S. Kristal, J. Nutr. 131 (2001) 924S–932S.
- [8] M.S. Rashed, J. Chromatogr. B. Biomed. Sci. Appl. 758 (2001) 27–48.
- [9] O. Fiehn, J. Kopka, P. Dormann, T. Altmann, R.N. Trethewey, L. Willmitzer, Nat. Biotechnol. 18 (2000) 1157–1161.
- [10] L.Q. Pang, Q.L. Liang, Y.M. Wang, P. Li, G.A. Luo, J. Chromatogr. 1–2 (2008) 118–125.
- [11] H.Y. Zhang, G.A. Luo, Q.L. Liang, Y. Wang, H.H. Yang, Y.M. Wang, X.Y. Zheng, X.M. Song, C. Gong, T. Zhang, J.X. Wu, Exp. Neurol. 2 (2008) 515–521.
- [12] L. Eriksson, E. Johansson, N. Kettaneh-Wold, S. Wold, Umetrics AB Press, Malmo, Sweden, 1999.
- [13] W.L. Farrar, J.L. Humes, J. Immunol. 135 (1985) 1153–1159.
- [14] M.E. Pasqualini, M.A. Berra, M.P. Yurawecz, G. Repposi, A.R. Eynard, Curr. Nutri. Food Sci. 4 (2008) 161–175.
- [15] J.M. Cook-Moreau, Y.E. Hojeij, G. Barrière, H.C. Rabinovitch-Chable, K.S. Faucher, F.G. Sturtz, M.A. Rigaud, Immunology 122 (2007) 157–166.
- [16] L.A. Rosenthal, D.D. Taub, M.A. Moors, K.J. Blank, Immunopharmacology 24 (1992) 203–217.
- [17] M.E. Hamel, E.E. Eynon, H.F.J. Savelkoul, A. Oudenaren, A.M. Kruisbeek, Int. Immunol. 7 (1995) 1065–1077.
- [18] A.J. Jame, P.M. Lackie, A.M. Cazaly, I. Sayers, J.F. Penrose, S.T. Holgate, A.P. Sampson, Clin. Exp. Allergy 37 (2007) 880–892.
- [19] S.T. Holgate, M. Peters-Golden, R.A. Panettieri, W.R. Henderson, J. Allergy Clin. Immunol. 111 (2003) S18–S34.
- [20] S. Altraja, M. Kadai, E. Rekker, A. Altraja, Respir. Res. 9 (2008) 44.
- [21] T. Asakura, Y. Ishii, K. Chibana, T. Fukuda, J. Allergy Clin. Immunol. 114 (2004) 310–315.
- [22] K. Espinosa, Y. Bosse, J. Stankova, M. Rola-Pleszczynski, J. Allergy Clin. Immunol. 111 (2003) 1032–1040.
- [23] M.M. Kelly, J. Chakir, D. Vethanayagam, L.P. Boulet, M. Laviolette, J. Gaudie, P.M. O'Byrne, Chest 130 (2006) 741–753.
- [24] T.D. Penning, Curr. Pharm. Design 7 (2001) 163–179.